Synthesis, Structural Investigation, Antiphospholipases, Antiproteases and Antimicrobial Activities of 2-(4-hydroxy-3-methoxy-benzylidene)-6-methoxy-3,4-dihydro-2*H*-naphthalen-1-one and 4-(4-hydroxy-3-methoxy-phenyl)-8-methoxy-3,4,5,6-tetrahydro-1*H*-benzo[*h*]quinazoline-2-thione

[1,2]Nahed N. E. El-Sayed*, [1]Norah M. Almaneai, [3,4]Saied M. Soliman,
[5]Abir Ben Bacha and [6,7]Hazem A. Ghabbour
[1]*Department of Chemistry, College of Science, King Saud University,*
P.O. Box 22452, Riyadh 11451, Saudi Arabia.
[2]*National Organization for Drug Control and Research, Giza 35521, Egypt.*
[3]*Department of Chemistry, Rabigh College of Science and Art, King Abdulaziz University,*
P.O. Box 344, Rabigh 21911, Saudi Arabia;
[4]*Department of Chemistry, Faculty of Science, Alexandria University,*
P.O. Box 426, Ibrahimia, Alexandria 21321.
[5]*Biochemistry Department, Science College, King Saud University,*
P.O. Box 22452, Riyadh 11495, Saudi Arabia.
[6]*Department of Pharmaceutical Chemistry, College of Pharmacy, King Saud University,*
P. O. Box 2457, Riyadh 11451, Saudi Arabia.
[7]*Department of Medicinal Chemistry, Faculty of Pharmacy, University of Mansoura, Mansoura 35516, Egypt.*
nelsayed@ksu.edu.sa*

(Received on 13th June 2018, accepted in revised form 15th March 2019)

Summary: The molecular structure aspects of 2-(4-hydroxy-3-methoxy-benzylidene) -6-methoxy-3,4-dihydro-2*H*-naphthalen-1-one **3** and 4-(4-hydroxy-3-methoxy-phenyl)- 8-methoxy-3,4,5,6-tetrahydro-1*H*-benzo[*h*]quinazoline-2-thione **5** were investigated using spectroscopic analyses and DFT calculations. The calculated geometric parameters of the most stable isomer of **3** were in good agreement with the experimental data obtained from its X-ray analysis. On the basis of the HOMO and LUMO energies different reactivity descriptors such as chemical potential (μ), hardness (η), softness (S) and the electrophilicity index (ω) were calculated. It was found that the electrophilicity index (ω) of **3** is higher than that for **5** and the electronic chemical potential of **5** is higher than **3**. Also the hardness is lower for **3** than **5** which has larger number of electronegative atoms. The calculated ^{13}C and ^{1}H-NMR chemical shifts at the optimized geometry of the studied compounds were correlated well with the experimental data and showed high correlation coefficients (R^2). Both molecules were screened against some selected proteases, phospholipases, bacterial and fungal strains. Compound **3** demonstrated better antiproteases activity than **5** with its maximum inhibitory activity against trypsin. Interestingly, while **3** demonstrated moderate inhibition against all tested phospholipases, compound **5** was more potent in inhibiting the catalytic activities of DrG-IB and SG-IBsPLA$_2$s than oleanolic acid the reference antiphospholipase. Therefore, compound **5** may serve as a potential candidate for further development to identify therapeutic agents for treatment of diet induced obesity and diabetes. Antibacterial screening revealed that while **5** was completely inactive, **3** demonstrated promising inhibitory potential against some microbes with the lowest IC_{50} value against gram negative *Klebsiella pneumoniae ATCC 700603*.

Keywords: Quinazoline-2(1*H*)-thiones; 2-Arylidenetetralin-1-one; DFT calculations; Antiphospholipases; Antiproteases; Antimicrobial activity.

Introduction

Secretory PLA_2 ($sPLA_2$s) is a subgroup of phospholipase A_2 (PLA_2) superfamily involved in the regulation of a great variety of physiological events such as digestion, inflammation, tissue injury, atherosclerosis, host defense, reproduction and skin homoeostasis [1,2]. Likewise, it had become evident that proteases make a distinct contribution to various biological processes such cell differentiation, proliferation, replication and transcription of DNA, protein-protein interaction, immune response, maturation, fertilization, ovulation, bone formation, survival and programmed cell death, and the recycling of cellular proteins [3]. All of these enzymatic activities are critical to the progression of a number of serious diseases either directly or indirectly [4-14]. Also, it was reported that the secretions of both phospholipases and proteases are very well-known virulence characteristics in case of Candida infections [15]. Correspondingly, development of potent and selective inhibitors for the

*To whom all correspondence should be addressed.

management of these proteins is considered a highly remarkable aspect of drug discovery processes for therapeutic candidates to be used for the prevention and treatment of immunological complaints, inflammatory bowel disease (IBD), diet-induced diabetes and cancer or to provide protection from infectious microbes [16-20].

In this context, chalcones and their analogues are considered as privileged candidates for these purposes due to their wide spectrum of pharmacological activities including antimitotic [21], anti-inflammatory [22], antioxidant [23], analgesic [24], Angiotensin I-Converting Enzyme (ACE) inhibitors [25], anti-protozoal [26], anti-histaminic [27], antibacterial [28] antifungal [29] and anticancer agents [30]. Moreover, quinazoline-2(1*H*)-thiones and their annealed derivatives are attractive drug scaffolds found in many of the synthetically developed biologically active heterocyclic compounds such as the Bcl-$x_L$inhibitors [31], cathepsin B and cathepsin H inhibitors [32], antimicrobials [33,34], cytotoxic and anti-HIV candidates [35].

Considering, the aforementioned facts which coupled with our interest in the synthesis of bioactive molecules as phospholipases and proteases inhibitors and antimicrobial agents [36,37], we report herein the synthesis, characterization of 2-arylidenetetralin-1-one **3** and the new tetrahydrobenzo[*h*]quinazoline-2-thione derivative **5**. The structures of the two compounds were investigated using density function theory methods. The natural populations of the atomic charges were calculated using the natural bond orbital (NBO) method and correlated to the data obtained from the X-ray structure of **3**. The reactivity of the two compounds toward electron transfer process have been determined using Frontier molecular orbitals (FMOs). NBO analyses were used for studying the intra-molecular charge transfer (ICT) interactions taking place in the studied molecular systems. The NMR chemical shifts were calculated using the gauge including atomic orbital (GIAO) method and correlated to the experimental data. Moreover, in *vitro* antiphospholipases and antiproteases activities of the two compounds were investigated to explore their potential for controlling inflammation, inflammation associated diseases and diet-induced obesity and diabetes as well. Besides, the antimicrobial activities of the studied compounds were evaluated against two pathogenic plant fungi and fourteen strains of gram positive and gram negative bacteria with the aim to develop new agents capable of inhibiting resistant bacteria and fungi.

Experimental

Synthesis

Melting points were determined on a Gallenkamp melting point apparatus and are uncorrected. Infrared spectra were recorded on a Perkin Elmer 1600 FTIR spectrophotometer. NMR spectra were recorded on a 1-Ascend Bruker NMR spectrometer operating at 850 MHz for ^{1}H and 213 MHz for ^{13}C or on a Bruker DPX 400 spectrometer operating at 400 MHz for ^{1}H and at 100 MHz for ^{13}C at 25 °C. All chemical shifts (δ) are reported in ppm relative to the internal standard tetramethylsilane. Coupling constants (*J*) are reported in Hz. Multiplicity in ^{1}H-NMR is reported as singlet (s), doublet (d), double of doublets (dd), triplet (t), and multiplet (m). Mass spectra were recorded on a ShimadzuQp-2010 Plus mass spectrometer works using electron ionization Mode (EI). Elemental analyses were performed on Perkin Elmer 2400 elemental analyzer; CHN mode and the values found were within ±0.3% of the theoretical values. All chemical reagents were commercially available and used without further purification.

2-(4-Hydroxy-3-methoxy-benzylidene)-6-methoxy-3,4-dihydro-2H-naphthalen-1-one (**3**)[38]

To a stirred solution of 6-methoxy-1-tetralone **1** (4.93 g, 0.028 mol) in conc. HCl (37%, 28 mL) and glacial acetic acid (28 mL) at 0 °C, vanillin **2** (4.3 g, 0.028mol) was added. The resulting mixture was further stirred at this temperature for 3 h, then at room temperature for 18 h. Diethyl ether was added and the ethereal layer was discarded. The remaining residue was treated with water/ice mixture, and the separated solid was filtered off and recrystallized from ethanol/petroleum ether to afford the 2-arylidene tetralin-1-one derivative **3** (50 %) as red crystals, m.p. 112-115 °C; ν_{max} (KBr)/cm^{-1} 3431, 3177, 2940, 2838, 1638, 1597, 1559, 1520, 1443, 1425, 1390, 1317, 1253, 1165; δ_H (400 MHz; $CDCl_3$) 2.92 (2 H, t, *J*=6.0, CH_2), 3.13 (2 H, t, *J* = 6.0, CH_2), 3.87 (3H, s, OCH_3), 3.92 (3H, s, OCH_3), 6.70 (1H, d, *J*= 2.6, CH-Ar), 6.87 (1H, dd, *J*= 8.5, 2.6, CH-Ar), 6.95-6.96 (2H, m, 2 × CH-Ar), 7.02 (1H, dd, *J*= 7.7, 1.7, CH-Ar), 7.78 (1H, s, CH=C_q-CO), 8.10 (1H, d, *J*= 8.5, CH-Ar); δ_C (100 MHz; $CDCl_3$) 27.28 (CH_2), 29.18 (CH_2), 55.40 (OCH_3), 55.94 (OCH_3), 112.21, 112.73, 113.21, 114.39, 123.64, 127.14, 128.32, 130.66, 133.70, 136.33, 145.51, 146.24, 163.46 (6 × CH-Ar, CH=C_q-CO and 6 × C_q-Ar), 186.71 (C=O); MS (EI) *m/z* (%) [M^+ + 1] 311.15 (14.29), [M^+] 310.15 (69.06), 309.15 (100.00), 295.10 (9.67), 294.10 (15.64), 293.15 (12.54), 279.10 (11.79),

137.10 (7.88), 125.15 (4.63), 120.10 (3.11), 89.05 (3.88), 77.00 (4.84). Anal. Calcd. for $C_{19}H_{18}O_4$ (310.34): C, 73.53; H, 5.85; Found: C, 73.78; H, 5.96.

4-(4-Hydroxy-3-methoxy-phenyl)-8-methoxy-3,4,5,6-tetrahydro-1H-benzo[h]quinazoline-2-thione (**5**)

A mixture of 6-methoxy-1-tetralone **1** (0.46 g, 0.0026 mol), vanillin **2** (0.4g, 0.0026 mol) and thiourea **4** (0.32 g, 0.0042 mol, 1.62 equiv.) in ethanol (20 mL) containing (1 mL) of conc. HCl (37%) was refluxed for 27 h. The reaction mixture was concentrated under reduced pressure to afford the crude product. Crystallization from chloroform afforded **5** (45 %) as a yellow powder, m.p. 253-255 °C; ν_{max} (KBr)/cm^{-1} 3402, 3199, 3114, 2996, 1578, 1501, 1461, 1358, 1307, 1256, 1215, 1173, 1088, 1031, 914, 857, 828, 780, 743, 684, 497; δ_H (850 MHz; DMSO-d_6) 1.85-1.88 (1H, m, CH-aliph), 2.12-2.15 (1H, m, CH-aliph), 2.58-2.62 (1H, m, CH-aliph), 2.68-2.72 (1H, m, CH-aliph), 3.74 (3H, s, OCH_3), 3.75 (3H, s, OCH_3), 4.82 (1H, s, CH-pyrimidine), 6.70 (1H, dd, *J*= 6.5, 1.5, CH-Ar), 6.76-6.78 (3H, m, 3 × CH-Ar), 6.88 (1H, d, *J*= 1.7, CH-Ar), 7.61 (1H, d, *J*= 8.5, CH-Ar), 8.91 (1H, s, NH), 9.05 (1H, s, NH), 9.60 (1H, s, OH); δ_C (312 MHz; DMSO-d_6) 23.58 (CH_2), 27.77 (CH_2), 55.07 (OCH_3), 55.58 (OCH_3), 58.17 (CH-pyrimidine), 108.77, 110.75, 111.41, 113.88, 115.50, 119.38, 120.65, 122.92, 126.32, 133.91, 137.48, 146.27, 147.48, 158.77 (6 × CH-Ar, 6 × C_q-Ar, 2 × C_q-pyrimidine), 173.77 (C=S); MS (EI) *m/z* (%) [M^+ + 1] 369.10 (25.58), [M^+] 368.15 (100.00), 367.15 (53.86), 335.15 (16.51), 308.15 (10.49), 246.10 (16.14), 245.10 (98.68), 184.05 (9.17), 152.10 (3.19), 137.15 (3.12), 125.00 (3.49), 115.10 (3.92), 109.05 (3.29), 97.15 (3.65), 83.10 (4.00), 69.05 (5.08), 55.05 (5.94).Anal. Calcd. for $C_{20}H_{20}N_2O_3S$ (368.45): C, 65.20; H, 5.47; N, 7.60; Found: C, 65.49; H, 5.63; N, 7.82.

Calculation methods

The DFT/B3LYP method has been validated to give results close to those for the more computationally expensive MP2 method for molecular geometries and frequency calculations [39,40] Consequently, the DFT/B3LYP method at 6-31G(d,p) basis set as implemented in Gaussian 03 program package [41,42] was used to calculate the equilibrium molecular geometries of the possible isomers of the titled compounds (Scheme-1). For all computations, frequency calculations were performed using the same level of theory. These frequency calculations showed that all structures were stationary points in the geometry optimization procedures and none showed imaginary frequencies in the vibrational analyses. On the basis of the principle of statistical thermodynamics [43], entropy (S), enthalpy (H) and Gibbs free energy (G) of the isomers under standard conditions of T=298.15 K and P= 1 atm have been obtained. The NMR chemical shifts were computed using the GIAO method [44, 45].The natural bond orbital (NBO) calculations were performed using NBO 3.1 program of the Gaussian 03W package at the DFT/B3LYP level in order to understand the various orbital interactions between the filled orbitals of one subsystem and vacant orbitals of another subsystem, which are considered as a measure of the intermolecular delocalization or hyperconjugation [46].

Biological testing

$sPLA_2$ inhibition assay [47]

The substrate consisted of 3.5 mM lecithin in a mixture of 3 mM Sodium Taurodeoxycholate (NaTDC), 100 mM NaCl, 10 mM $CaCl_2$ and 0.055 mM red phenol as a colorimetric indicator dissolved in 100 mL of H_2O. The pH of the reaction mixture was adjusted to 7.6. The Human group IIA (hG-IIA), the dromedary group V (DrG-V), IIA (DrG-IIA), and IB (Dr-IB) $sPLA_2$ and the stingray group V (SG-V), IIA (SG-IIA), IB (SG-IB) $sPLA_2$ were solubilized in 10% acetonitrile at a concentration of 0.02 µg/µl;. A volume of 10 µL of these PLA_2 solutions was incubated with 10 µL of each compound dissolved in 100 % DMSO for 20 min at room temperature. Then, 1 mL of the $sPLA_2$ substrate was added, and the kinetic progress of the hydrolysis reaction was followed for a duration of 5 min by reading the optical density at 558 nm. Oleanolic acid and DMSO were used as positive and negative control, respectively. The inhibition percentage was calculated by comparison with a control experiment (i.e. DMSO in the absence of the compound).

Proteases inhibition assay

Four commercially available proteases namely, proteinase K (Sigma-Aldrich, P2308), and that obtained from *Aspergillus oryzae* (Sigma-Aldrich, P6110), *Bacillus licheniformis* (Sigma-Aldrich, P4860) and *Bacillus sp.* (Sigma-Aldrich, P3111), and four proteases with therapeutic importance, namely, chymotrypsin (Sigma-Aldrich, C3142), collagenase (Sigma-Aldrich, C2674), thrombin (Sigma-Aldrich, T7513) and trypsin

(Sigma-Aldrich, T4799) were used to study the effects of the prepared compounds (dissolved in 100 % DMSO) on their enzymatic activities. Proteases assays were carried out by adopting the Kunitz caseinolytic method [48] using Hammerstein casein as the substrate. The respective protease inhibitor activity was assayed under the same conditions with the addition of the inhibitor (0.1 mg/mL) to the respective reaction mixture, preincubation for 10 min, and assaying the residual enzyme activity. A protease inhibitor unit is defined as the amount of protease inhibitor that was able to inhibit one unit of respective enzyme activity. The protease inhibitor activity has been expressed in terms of percent inhibition. Appropriate blanks for the enzyme, inhibitor, and the substrate were also included in the assay.

Antibacterial Activity

Culture of bacterial strains preparation

Pure standard microbial isolates collected from King Khaled University Hospital were tested in this study; including *Staphylococcus aureus* ATCC 25923, *Staphylococcus aureus* Ala 1, Methicillin resistant *Staphylococcus aureus* ATCC3345, *Bacillus subtilis* ATCC 6633, *Enterococcus faecalis* ATCC 29212, *Streptococcus pyogens*ATCC 19615, and *Streptococcus mutans* as gram positive, and *Escherichia coli* ATCC 25966, *Escherichia coli* ATCC 35218, *Pseudomonas aeruginosa* ATCC 27853, *Klebsiella pneumoniae* ATCC 700603, *Salmonella sp., Salmonella typhimurium* LT2 and *Serratia marcescens* as gram negative bacteria. Fresh cultures of each microorganism were grown on nutrient agar plates (Oxoid, UK), of which small inoculums were suspended in 5 mL of the nutrient broth for bacterial suspension preparation of 0.5MacFarland.

Antibacterial assay

Antimicrobial activity was assayed using the well diffusion technique according to the vanden Berghe and Vlietinck protocol [49]. Briefly, small inoculums of each of the prepared microbial suspensions were loaded on the surface of sterile Muller Hinton agar plates (Oxoid) with sterile cotton swabs. The loaded plates were then equidistantly perforated using a sterile 6mm diameter cork borer. Next, 70 µL of each compound (1 mg/ml, dissolved in 100% DMSO) was loaded in the appropriate well. The plates were allowed to rest for 30 min. at room temperature and then incubated at 37°C for 18-24 h. Antimicrobial activity was determined by measuring the inhibition zone. All tests were performed in duplicates and means of inhibition zones were recorded in mm. Tetracycline, Vancomycin and Gentamicin were used as positive drugs while DMSO was used as the negative control.

Determination of minimal inhibitory concentration (MIC)

Micro-well dilution method was performed to determine the MIC values, which represent the lowest concentrations of the studied chemical compounds that are capable of completely inhibiting the visible growth of bacteria [50]. Dilutions series of compound **3** dissolved in 100% DMSO were prepared in a 96-well plate. Each well contained 50 µL of the diluted compound, 10 µL of inoculums (10^6 CFU/mL) and 40 µL of the growth medium. Dimethyl sulfoxide and tetracycline were used as negative and positive controls respectively. Subsequently, the plate was covered with another sterile plate and incubated for 24 h at 37°C. Then, 40 µL of freshly prepared MTT dye (3-(4,5-dimethylthiazol-2-yl)-2,5-diphenyltetrazolium bromide) (0.5 mg/mL) was added to each well and incubated for 30 min. The biologically active bacteria were indicated by the change to red color. The MIC was taken to the well, where no change of color of MTT was observed. The experiments to determine the MIC values were performed in triplicate.

Determination of the IC_{50} values (concentration eliciting 50% inhibitory effect for bacterial activity)

Bacterial viability was investigated by measuring the colony-forming ability (CFU) of bacteria incubated in the presence or absence of compound **3** (dissolved in 100% DMSO) for different times. The assay mixtures included 2×10^7 CFU/mL in sterile BHI supplemented with the appropriate amounts of the compound were incubated for 60 min with shaking at 37 °C. At different intervals, aliquots were withdrawn and serially diluted into sterile BHI. To determine the bacterial viability by colony counting, samples were streaked onto media agar plates and incubated at 37 °C for 24h. The bactericidal effect of compound **3** was expressed as the residual number of CFU with respect to the initial inoculums and the IC_{50} value corresponding to the compound concentration capable to inhibit 50% of the initial inoculums. DMSO was used as the negative control. The experiments to determine IC_{50} values were performed in triplicate.

Antifungal Activity

Fungal culture and media preparation

Two fungal species namely *Fusarium* sp. and *Alternaria alternate* were isolated from plants and identified by the Department of Mycology at king Saud University. Both species were cultured, purified and maintained on Sabouraud dextrose agar (Oxoid) for testing the antifungal activities of the chemical compounds prepared in study.

Antifungal assay

The antifungal assays for compounds **3** and **5** were performed by measuring the diameter growth of the fungal strains using disc the diffusion technique [51]. 100 µL of each of the chemical compounds (1mg/ml in 100% DMSO) was inoculated in the center of a sterile Petri dish and then mixed with 20 mL of the Sabouraud dextrose agar. The plates were allowed to solidify and subsequently, 5 mm sized-disc was cut from each of the test fungi *Fusarium* and *Alternaria*, using a sterile cork borer. The disc was placed upside down at the center of the agar- chemical compound plates and incubated for 5 days at 28 °C. The control plates (containing the experimented fungi and DMSO without the chemical compound) were prepared for comparing the inhibitory effects of compounds **3** and **5**. Tests were performed in duplicates. The growth of each of the fungal strains was measured and determined as the mean diameter growth in mm.

Results and Discussion

Chemistry

The Knoevenagel condensation between 6-methoxy-1-tetralone **1** and vanillin **2** under acidic catalysis by adopting procedures reported by Du and co-workers [38] afforded 2-arylidenetetralin-1-one derivative **3** as portrayed in Scheme-1. Next, cyclocondensation of **3** with thiourea **4** was attempted under basic catalysis according to the reported method [52] with the aim to obtain tetrahydrobenzo[*h*]quinazoline-2-thione derivative **5**. However, after 27 h of refluxing the reaction mixture, the TLC analysis indicated formation of a complex mixture of compounds which was very difficult to separate. The same result was obtained by using the modified protocol under acidic conditions [53]. One possible reason for this result in a strong acidic medium is the protonation of carbonyl oxygen atom of enone moiety in compound **3** that resulted in increasing the electrophilic character of the β-conjugated position of intermediate **A** which therefore, could be subjected to nucleophilic attack either by nitrogen or sulfur atoms of thiourea molecule. Subsequent intramolecular cyclization would furnish the desired Biginelli product **5** having benzo[*h*]quinazoline-2-thione core or its isomeric product **6** incorporating 2-amino-1,3-thiazine ring as documented in the literature [54] as depicted in Scheme-2.

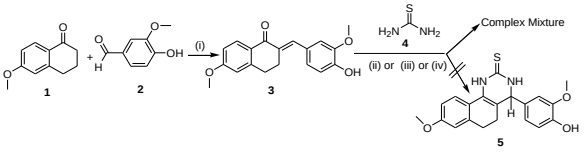

Scheme-1: Synthesis and attempts of cyclocondensation of 2-arylidenetetralin-1-one **3**

Reagents and conditions: (i) Compound **1**, conc. HCl, AcOH, 0 °C, compound **2**, stirring 3 h at 0 °C, overnight at r. t.; (ii) Compound **3** (0.6 g, 0.0019 mol), compound **4** (0.14 g, 0.0019 mol), conc. HCl (1 mL), EtOH, reflux 27 h; (iii) Compound **3 (**0.6 g, 0.0019 mol), compound **4** (0.14 g, 0.0019 mol), conc. HCl (2 mL), CH_3CN, reflux 27 h; (iv) Compound **3** (0.5 g, 0.0016 mol), compound **4** (0.3 g, 0.0039 mol), KOH (0.33 g , 0.0058 mol), EtOH, reflux 27 h.

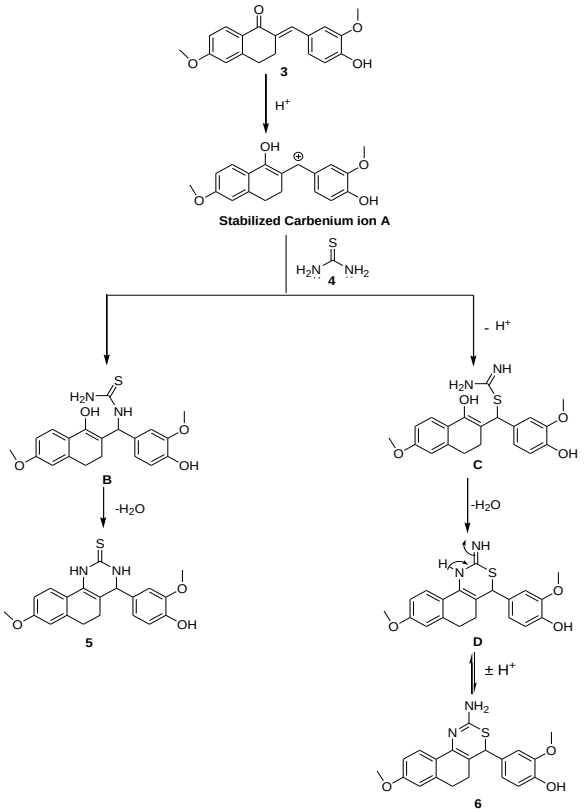

Scheme-2: The proposed mechanisms for formation of compounds **5** and **6**

Therefore, the one pot, three component synthesis using 6-methoxy-1-tetralone **1**, vanillin **2** and thiourea **4** under acidic conditions was the next optimal choice and it successfully led to the formation of the desired product **5** rather than the isomeric 2-amino-1,3-thiazine **6**, as shown in Scheme-3.

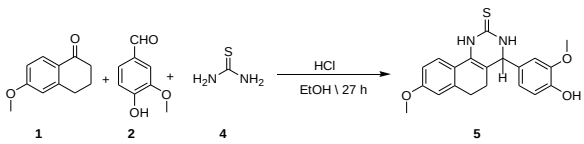

Scheme-3: One pot synthesis of compound **5.**

The assignment of the structure of 2-arylidene tetralin-1-one **3** was based on the following observations. The presence of an absorption band at ν_{max}= 1733 cm^{-1} in the IR spectrum attributed to the conjugated carbonyl group. The presence of only two triplet signals at δ 2.90 and 3.11 ppm in ^{1}H-NMR spectrum each integrating to two protons, corresponded to the two methylene groups of the 1-tetralone fragment. The appearance of a singlet signal at δ 7.76 ppm, integrating to one proton which was attributed to the β-methine proton of the characteristic α,β-enone functionality. Furthermore, the ^{13}C-NMR spectrum revealed the presence of only two methylene groups at δ 27.28 and 29.18 ppm and the characteristic carbonyl group at δ 186.71 ppm. Also the mass spectrum (EI) of compound **3** indicated the presence of the expected molecular ion [M^+ + 1] at *m/z* 311.15 (14.29%) for $C_{19}H_{18}O_4$ and the base peak was observed at *m/z* 309.15 (100.00%).

Analogously, the assignment of the structure of the tetrahydrobenzo[*h*]quinazoline-2-thione derivative **5** was based on the following observations. The emergence of an absorption band at ν_{max}= 1173 cm^{-1} due to C=S functionality in the IR spectrum. In the ^{1}H-NMR spectrum, the two methylene groups of the tetralone core exhibited complicated splitting patterns because of generation of the new stereogenic center at C-4 in the tetrahydro-1*H*-benzo[*h*]quinazoline-2-thione scaffold and the proton at this center was demonstrated by a one proton singlet spectral line at δ 4.82 ppm. Moreover, the presence of two singlet spectral lines at δ 8.93 and 9.05 ppm corresponded to the two NH groups proved the formation of structure **5** rather than its isomeric 2-amino-1,3-thiazine derivative **6**. The ^{13}C-NMR spectrum also confirmed the formation of tetrahydro-1*H*-benzo[*h*]quinazoline-2-thione derivative **5** as indicated by the presence of a new spectral line at δ 58.17 ppm which would be attributed to the methine carbon of the pyrimidine ring and the presence of a new spectral line at δ 173.77 ppm arising from the thiocarbonyl group. The mass spectrum (EI) showed the molecular ion [M^+ + 1] at *m/z* 369.10 (25.58%) for $C_{20}H_{20}N_2O_3S$ and the base peak [M^+] was observed at *m/z* 368.15 (100.00%).

Structural investigation

Stabilities and energetic

The optimized structures of compounds **3** and **5** are shown in Fig 1. The total energies (E_{tot}), zero point vibrational energies (ZPVE), corrected energies (E_{corr}) and the thermodynamic parameters of all suggested isomers are given in Table-1. For compound **3**, it is evident that, the **T11** is more stable than **T12** by 3.08 kcal/mol. The latter has a higher energy because of the steric effect. On other hand, for compound **5** the thione tautomer is predicted to be more stable than either of the two thiol isomers. The **T21** form (thione) is more stable than **T22** and **T23** by 16.99 and 14.29 kcal/mol, respectively. As a result the order of tautomeric stability of the suggested isomers of **5** is **T21** > **T23** > **T22**. The thermodynamic parameters indicates that the conversion of any of the less stable isomers to the most stable one is an exothermic process with negative ΔH. Also, the **T11** and **T12** isomers are thermodynamically more stable than the others as indicated from their negative ΔG values.

Table-1: Energies and thermodynamic parameters of the different isomers of 3 and 5.

	3		**5**		
Cpd #	**T11**	**T12**	**T21**	**T22**	**T23**
E_{tot}(a.u)	**-1035.7580**	**-1035.7532**	**-1507.5621**	**-1507.5306**	**-1507.5351**
ZPVE(a.u)	**0.3311**	**0.3312**	**0.3702**	**0.3659**	**0.3660**
E_{corr}(a.u)	**-1035.4270**	**-1035.4220**	**-1507.1918**	**-1507.1647**	**-1507.1691**
ΔE (kcal/mol)		**3.0809**		**16.9944**	**14.2884**
H (a.u)	**-1035.4057**	**-1035.4008**	**-1507.1676**	**-1507.1401**	**-1507.1445**
ΔH(kcal/mol)[a]		**-3.0378**		**-17.2465**	**-14.5356**
G (a.u)	**-1035.4768**	**-1035.4720**	**-1507.2464**	**-1507.2195**	**-1507.2237**
ΔG (kcal/mol)[a]		**-2.9882**		**-16.8624**	**-14.2765**
S (cal. $mol^{-1}K^{-1}$)	**149.7080**	**149.8740**	**165.8340**	**167.1210**	**166.7020**

[a] The difference between the most stable isomer and the less stable one

Optimized geometry

The optimized geometric parameters of the studied compounds are given in Table-2. The calculated bond distances of the most stable isomers of compound **3** are in agreement with the reported X-ray structure (CCDC 1459326) [55] and the calculated bond distances are deviated very slightly from the experimental data. The maximum error doesn't exceed 0.018 Å for the C27-C29 bond. Fig. 2 shows the correlations between the calculated and experimental bond distances of **3**. The correlation coefficients (R^2= 0.942-0.981) indicates that there is

a good agreement between the calculated and experimental structures.

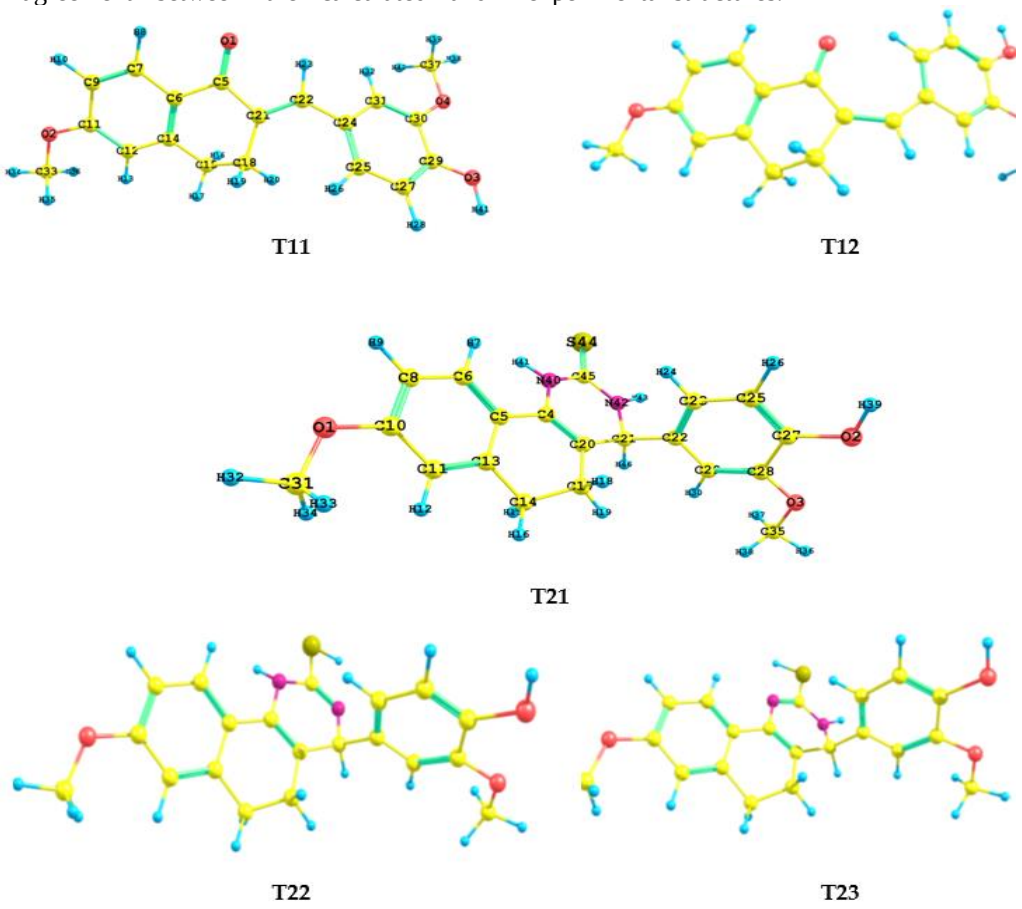

Fig. 1: Optimized structures of the suggested isomers of compounds **3** and **5**.

Table-2: Calculated bond distances of the studied compounds.

Parameter	3		5	
R(1-5)	1.231	1.243	R(1-10)	1.363
R(2-11)	1.361	1.360	R(1-31)	1.420
R(2-33)	1.420	1.438	R(2-27)	1.364
R(3-29)	1.362	1.364	R(3-28)	1.363
R(4-30)	1.362	1.366	R(3-35)	1.418
R(4-37)	1.419	1.428	R(4-5)	1.475
R(5-6)	1.487	1.475	R(4-20)	1.350
R(5-21)	1.500	1.483	R(4-40)	1.403
R(6-7)	1.407	1.403	R(5-6)	1.405
R(6-14)	1.405	1.402	R(5-13)	1.409
R(7-9)	1.382	1.371	R(6-8)	1.388
R(9-11)	1.407	1.400	R(8-10)	1.401
R(11-12)	1.400	1.388	R(10-11)	1.401
R(12-14)	1.399	1.394	R(11-13)	1.395
R(14-15)	1.510	1.507	R(13-14)	1.513
R(15-18)	1.537	1.532	R(14-17)	1.534
R(18-21)	1.512	1.512	R(17-20)	1.509
R(21-22)	1.354	1.346	R(20-21)	1.511
R(22-24)	1.463	1.465	R(21-22)	1.530
R(24-25)	1.403	1.391	R(21-42)	1.471
R(24-31)	1.415	1.403	R(22-23)	1.394
R(25-27)	1.396	1.387	R(22-29)	1.403
R(27-29)	1.392	1.374	R(23-25)	1.396
R(29-30)	1.416	1.409	R(25-27)	1.393
R(30-31)	1.390	1.380	R(27-28)	1.413
			R(28-29)	1.396
			R(40-45)	1.366
			R(42-45)	1.352
			R(44-45)	1.684

[a] List of bond angles is given in the Supplementary data (Table S1).

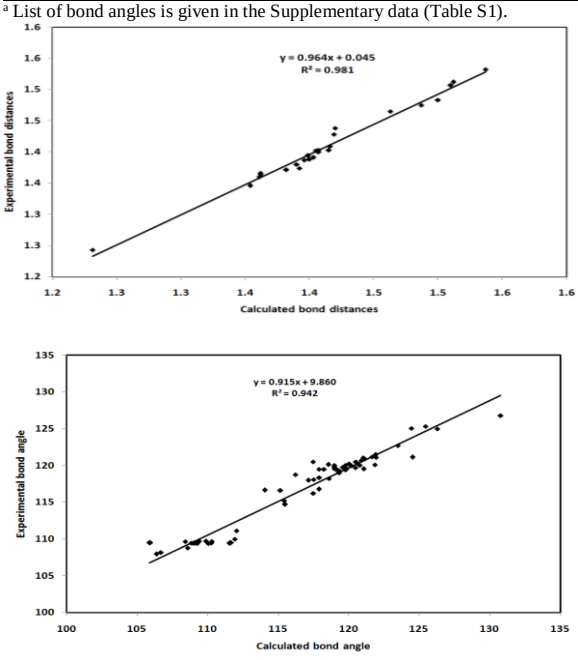

Fig. 2: Correlation graphs between the calculated and experimental geometric parameters of **3**.

Table-3: Calculated natural charges of compounds**3** and **5**.

3		5	
O1	**-0.5784**	**O1**	**-0.5158**
O2	**-0.5126**	**O2**	**-0.6804**
O3	**-0.6763**	**O3**	**-0.5089**
O4	**-0.5101**	**C4**	**0.1631**
C5	**0.5303**	**C5**	**-0.0976**
C6	**-0.1658**	**C6**	**-0.2122**
C7	**-0.1678**	**H7**	**0.2380**
H8	**0.2625**	**C8**	**-0.2739**
C9	**-0.2840**	**H9**	**0.2539**
H10	**0.2523**	**C10**	**0.3336**
C11	**0.3492**	**C11**	**-0.3135**
C12	**-0.3271**	**H12**	**0.2406**
H13	**0.2390**	**C13**	**0.0163**
C14	**0.0212**	**C14**	**-0.4687**
C15	**-0.4704**	**H15**	**0.2518**
H16	**0.2550**	**H16**	**0.2487**
H17	**0.2469**	**C17**	**-0.4711**
C18	**-0.4845**	**H18**	**0.2523**
H19	**0.2473**	**H19**	**0.2484**
H20	**0.2535**	**C20**	**-0.0649**
C21	**-0.1162**	**C21**	**-0.0688**
C22	**-0.1530**	**C22**	**-0.0734**
H23	**0.2565**	**C23**	**-0.2321**
C24	**-0.0891**	**H24**	**0.2500**
C25	**-0.2265**	**C25**	**-0.3029**
H26	**0.2426**	**H26**	**0.2365**
C27	**-0.3107**	**C27**	**0.2983**
H28	**0.2346**	**C28**	**0.2846**
C29	**0.3067**	**C29**	**-0.3086**
C30	**0.2805**	**H30**	**0.2390**
C1	**-0.2836**	**C31**	**-0.3288**
H32	**0.2452**	**H32**	**0.2344**
C33	**-0.3292**	**H33**	**0.2067**
H34	**0.2341**	**H34**	**0.2070**
H35	**0.2077**	**C35**	**-0.3270**
H36	**0.2080**	**H36**	**0.2350**
C37	**-0.3278**	**H37**	**0.2052**
H38	**0.2338**	**H38**	**0.2037**
H39	**0.2073**	**H39**	**0.4929**
H40	**0.2064**	**N40**	**-0.6118**
H41	**0.4927**	**H41**	**0.4493**
		N42	**-0.6202**
		H43	**0.4470**
		S44	**-0.2701**
		C45	**0.2713**
		H46	**0.2432**

Natural charges

The natural populations of the atomic charges were calculated using the natural bond orbital (NBO) method (Table-3). For both molecules, the most negative charge is located over the O-atoms, where the O-atom of the OH group has the highest negative charge. Also, the S-atom of **5** has a negative charge. Thus these sites are the most reactive to be attacked by an electrophile. They are also considered the most H-accepting sites. In contrast, the H-atoms are the most positive, where the OH proton is the most positive in both molecules. Also, the two NH protons in **5** have high positive charges. These protons are the most favored to be attacked by a nucleophilic species and are considered the most H-donating sites. These facts are revealed by distributions of the electron density over the molecular electrostatic potential of the studied molecules (Fig. 3). As shown in this Fig there is a clear red region, i.e. negative electron density, located over the O and S-atoms indicating that these sites are the most nucleophilic sites. In contrast, the blue regions of low electron density are located over the OH/NH protons indicating that these sites are most electrophilic sites. Furthermore, these are considered as the most reactive protons for H-bonding interactions which are in agreement with the X-ray structure of **3**.

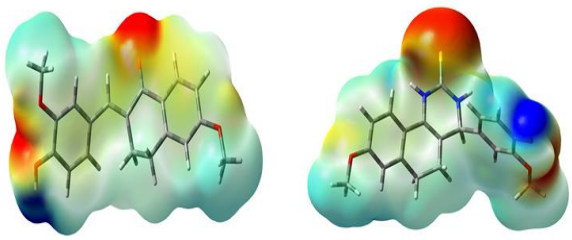

3 **5**

Fig. 3: MEP of the studied compounds.

Frontier molecular orbitals (FMOs)

The frontier molecular orbitals are the highest occupied (HOMO) and lowest unoccupied (LUMO) molecular orbitals which are related to the reactivity of compound toward electron transfer process. HOMO energy is a relative index for the ability of a molecule to donate electron. In contrast, the ability of a compound to accept electrons is related to its LUMO energy. Thus compounds having high energy HOMO and a low lying LUMO are considered as the most reactive electron donor and electron acceptor, respectively. Fig 4 shows the frontier molecular orbitals and their energies. The HOMO energies for **3** and **5** were calculated to be -5.4505eV and -5.2031 eV, respectively. It is evident that **5** is a better electron donor than **3**. In contrast, **5** have higher LUMO than **3** and hence the latter is considered a better electron acceptor with lower HOMO-LUMO gap of 3.8145 eV compared to 4.2477 eV for **5**. The orbital density of the HOMO and LUMO levels are mainly distributed over the π-system and partially over the heteroatom lone pairs. Hence, the HOMO-LUMO excitation could be described as π-π* excitation mixed with some n-π* transitions.

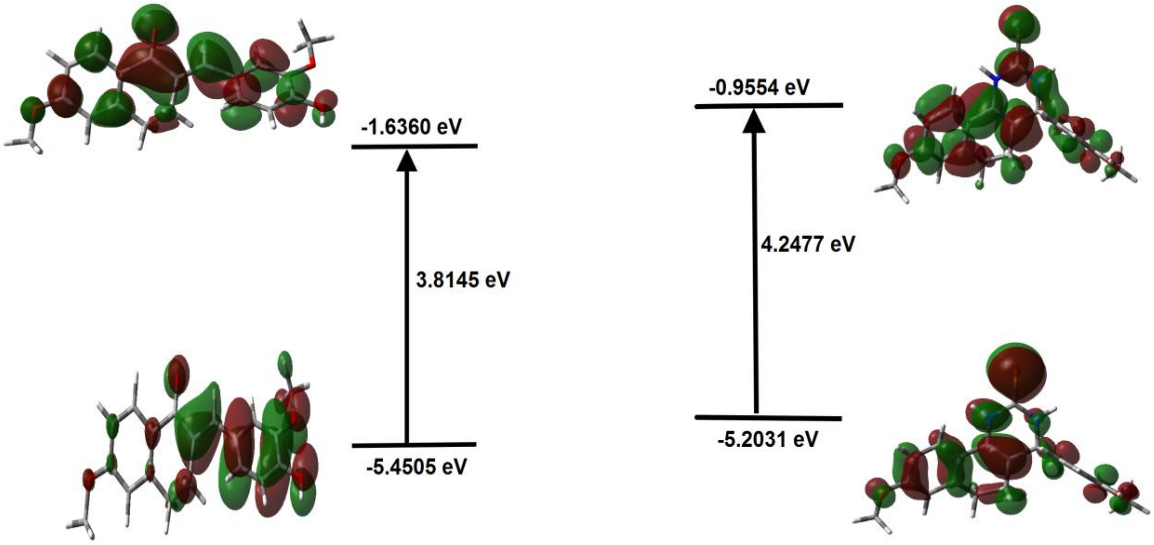

Fig. 4. The FMOs energy level diagram of the compounds **3** and **5**.

On the basis of the HOMO and LUMO energies, different reactivity descriptors such as chemical potential (μ), hardness (η), softness (S) and the electrophilicity index (ω) were calculated [56-62]. It is clear from the data shown in Table-4 that the electrophilicity index (ω) of **3** is higher than that for **5** indicating the higher electrophilic character of the former compared to the latter. In addition, soft systems are large and highly polarizable, while hard systems are relatively small and much less polarizable. The results indicated that, the hardness is lower for **3** than **5** which have larger number of electronegative atoms. Moreover, the electronic chemical potential of **5** is higher than **3** indicating the more ease of electron transfer from the former than the latter. These results agree with the HOMO and LUMO energies discussed above.

Table-4: The reactivity parameters of **3** and **5**

Parameter	3	5
μ	-3.5433	-3.0793
η	1.9073	2.1239
S	0.2622	0.2354
ω	3.2913	2.2322

Natural bond orbital (NBO) analysis

The second order perturbation energy analysis is one of the most important NBO features used for studying the intra- and intermolecular charge transfer (ICT) interactions taking place in molecular systems. The stabilization energy $E^{(2)}$ obtained from this analysis sheds light on the stabilization of the system due electron delocalization processes. Many intramolecular charge transfer delocalization processes such as π→π*, n→π* and n→σ* that occurred in the studied molecules have been listed in Table-5. Within the organic skeleton of the molecule, the system is stabilized by strong π→π* electron delocalization from the filled BD(2)C-C to the empty antibonding BD*(2)C-C NBOs, which stabilizes the system by up to 24 kcal/mol for both compounds. For **3**, some BD(2)C-C→ BD*(2)C-C ICT interactions were detected while **5** didn't show any BD(2)C-C→ BD*(2)C-S ICT interactions. On other hand, the n→π* ICT stabilization energies of up to 32.47 kcal/mol were detected for **3**. Interestingly, compound **5** shows a very strong electron delocalization from the LP(1)N filled NBOs to the empty BD*(1)S44-C45 with stabilization energy $E^{(2)}$ ranging from 70.55 to 81.81 kcal/mol. In contrast, the LP(2)S44→ BD*(1)N40-C45 interactions are weaker, which indicates that the BD*(1)S44-C45 antibonding natural orbitals are better electron acceptors than the BD*(1)N40-C45 one. Generally, the n→π* ICT interactions are stronger than the n→σ* ones for both compounds.

Moreover, the electron density (ED) of the donor (i) and acceptor (j) NBOs included in the ICT interactions are listed in the same table. As can be seen that the electron density of all the occupied π- and LP-type as NBOs donor orbitals are less than 2.00000 e; for a non-conjugated system such as ethanol molecule. In contrast, the acceptor π* and σ* acceptor NBOs are increased more than 0.00000 e in absence of any ICT transfer. The strong lowering the ED of the former and the significant increase in the

ED of the latter indicated the strong ICT interactions in the studied systems.

Table-5: Donor (NBO_i)→acceptor (NBO_j) interactions and their stabilization energies deduced from the second order perturbation theory[a].

3					5				
NBO_i	ED(i) e	NBO_j	ED(j) e	$E^{(2)}$	NBO_i	ED(i) e	NBO_j	ED (j) e	$E^{(2)}$
BD(2)C6-C14	1.63576	BD*(2)O1-C5	0.22215	21.33	BD(2)C4-C20	1.88896	BD*(2)C5-C6	0.41245	10.91
BD(2)C6-C14	1.63576	BD*(2)C7-C9	0.27301	21.65	BD(2)C5-C6	1.64940	BD*(2)C4-C20	0.21572	14.35
BD(2)C6-C14	1.63576	BD*(2)C11-C12	0.38944	16.21	BD(2)C5-C6	1.64940	BD*(2)C8-C10	0.39672	18.43
BD(2)C7-C9	1.70665	BD*(2)C6-C14	0.38247	15.27	BD(2)C5-C6	1.64940	BD*(2)C11-C13	0.35494	23.35
BD(2)C7-C9	1.70665	BD*(2)C11-C12	0.38944	23.51	BD(2)C8-C10	1.61656	BD*(2)C5-C6	0.41245	23.51
BD(2)C11-C12	1.65802	BD*(2)C7-C9	0.27301	13.69	BD(2)C8-C10	1.61656	BD*(2)C11-C13	0.35494	17.14
BD(2)C11-C12	1.65802	BD*(2)C6-C14	0.38247	23.98	BD(2)C11-C13	1.69132	BD*(2)C5-C6	0.41245	16.13
BD(2)C11-C12	1.65802	BD*(2)O1-C5	0.22215	20.06	BD(2)C11-C13	1.69132	BD*(2)C8-C10	0.39672	23.21
BD(2)C24-C25	1.97377	BD*(2)C21-C22	0.12734	12.01	BD(2)C22-C23	1.68835	BD*(2)C25-C27	0.38580	18.95
BD(2)C24-C25	1.97377	BD*(2)C27-C29	0.38557	19.61	BD(2)C22-C23	1.68835	BD*(2)C28-C29	0.39685	19.19
BD(2)C24-C25	1.97377	BD*(2)C30-C31	0.36668	18.52	BD(2)C25-C27	1.68630	BD*(2)C22-C23	0.36890	19.62
BD(2)C27-C29	1.68509	BD*(2)C24-C25	0.39030	19.42	BD(2)C25-C27	1.68630	BD*(2)C28-C29	0.39685	18.05
BD(2)C27-C29	1.68509	BD*(2)C30-C31	0.36668	17.03	BD(2)C28-C29	1.69661	BD*(2)C22-C23	0.36890	19.21
BD(2)C30-C31	1.70839	BD*(2)C24-C25	0.39030	17.54	BD(2)C28-C29	1.69661	BD*(2)C25-C27	0.38580	18.22
BD(2)C30-C31	1.70839	BD*(2)C27-C29	0.38557	18.42	LP(2)O1	1.83578	BD*(2)C8-C10	0.39672	28.42
LP(2)O1	1.88375	BD*(1)C5-C6	0.06151	18.88	LP(2)O2	1.86997	BD*(2)C25-C27	0.38580	29.16
LP(2)O1	1.88375	BD*(1)C5-C21	0.06637	19.41	LP(2)O3	1.83937	BD*(2)C28-C29	0.39685	30.73
LP(2)O2	1.82885	BD*(2)C11-C12	0.38944	32.47	LP(1)N40	1.67001	BD*(2)C4-C20	0.21572	32.82
LP(2)O3	1.86441	BD*(2)C27-C29	0.38557	29.66	LP(1)N40	1.67001	BD*(1)S44-C45	0.51353	70.55
LP(2)O4	1.83969	BD*(2)C30-C31	0.36668	30.90	LP(1)N42	1.67934	BD*(1)S44-C45	0.51353	81.81
					LP(2)S44	1.88782	BD*(1)N40-C45	0.05510	10.37
					LP(2)S44	1.88782	BD*(1)N42-C45	0.05510	10.50

[a] BD(2) = π; LP=lone pair (n); BD*(1) = σ* and BD*(2)=π*

Table-6: Calculated and experimental chemical shifts of the most stable isomers of the studied compounds.

3	Calc.	Exp.	5	Calc.	Exp.
C 5	177.18	186.71	C 4	123.84	126.32
C 6	124.70	128.32	C 5	117.96	122.92
C 7	127.43	130.66	C 6	116.25	120.65
C 9	111.73	113.21	C 8	111.37	115.50
C 11	156.15	163.46	C 10	153.31	158.77
C 12	103.51	112.73	C 11	105.59	110.75
C 14	139.89	145.50	C 13	134.07	137.48
C 15	31.77	29.18	C 14	31.70	27.77
C 18	30.07	27.28	C 17	26.69	23.58
C 21	128.96	133.70	C 20	103.92	108.77
C 22	134.98	136.33	C 21	64.40	58.21
C 24	125.83	127.14	C 22	130.43	133.91
C 25	116.30	123.64	C 23	115.69	119.38
C 27	108.66	112.21	C 25	110.75	113.88
C 29	141.87	146.01	C 27	141.17	146.27
C 30	142.83	146.24	C 28	141.80	147.48
C 31	111.72	114.39	C 29	106.70	111.41
C 33	52.55	55.40	C 31	52.52	55.58
C 37	52.62	55.94	C 35	52.45	55.07
H 8	8.28	8.10	C 45	170.35	173.77
H 10	6.87	6.87	H 7	7.05	7.61
H 13	6.33	6.70	H 9	6.82	6.76
H 16	2.93	3.13	H 12	6.37	6.71
H 17	2.40	2.92	H 15	2.86	2.70
H 19	2.77	2.92	H 16	2.22	2.60
H 20	3.08	3.13	H 18	1.96	2.14
H 23	7.88	7.78	H 19	1.47	1.87
H 26	6.86	7.02	H 24	7.03	6.88
H 28	6.34	6.96	H 26	6.45	6.77
H 32	6.65	6.95	H 30	6.31	6.78
H 34	3.96	3.87	H 32	3.92	3.74
H 35	3.61	3.87	H 33	3.56	3.74
H 36	3.61	3.87	H 34	3.55	3.74
H 38	4.03	3.92	H 36	4.03	3.75
H 39	3.62	3.92	H 37	3.55	3.75
H 40	3.60	3.92	H 38	3.52	3.75
H 41	3.48	---	H 39	3.36	9.62
			H 41	6.58	9.05
			H 43	5.30	8.93
			H 46	4.82	4.82

NMR

The NMR chemical shifts were calculated using the same level of theory at the optimized geometry of the studied compounds. The chemical shifts for the C and H-atoms were obtained on the δ-scale with respect to TMS as reference. The corresponding calculated and experimental chemical shifts for the hydrogen and carbon atoms are given in Table-6. The calculated chemical shift values are found to be in good agreement with the experimental data, except for the NH and OH protons. These protons are labile in solution and strongly involved in solute-solvent interactions, which explains the significant differences between the calculated and experimental values of these protons. The correlations between the experimental and calculated chemical shifts for the most stable isomers are shown in Fig. 5. The relationships between the calculated and experimental chemical shifts are linear. The correlation coefficients are high, which indicates that the method used to predict the NMR chemical shifts is highly accurate.

Biological evaluation

Phospholipases inhibitory screening

The inhibitory effects of the studied compounds were examined against several G-IIA and GV $sPLA_2$s and two GIB $sPLA_2$s.

As shown in Fig 6, although 2-arylidene tetralin-1-one **3** is more potent than compound **5**, it exhibits moderate inhibitory activity against proinflammatory GIIA and GV $sPLA_2$s compared to oleanolic acid which is used as the reference phospholipases inhibitor. Interestingly, compound **5**

is more potent than both of compound **3** and oleanolic acid in inhibiting the two types of GIB sPLA$_2$s. This implies that compound **5** might serve as a potential candidate for treatment of diet induced obesity and diabetes [8].

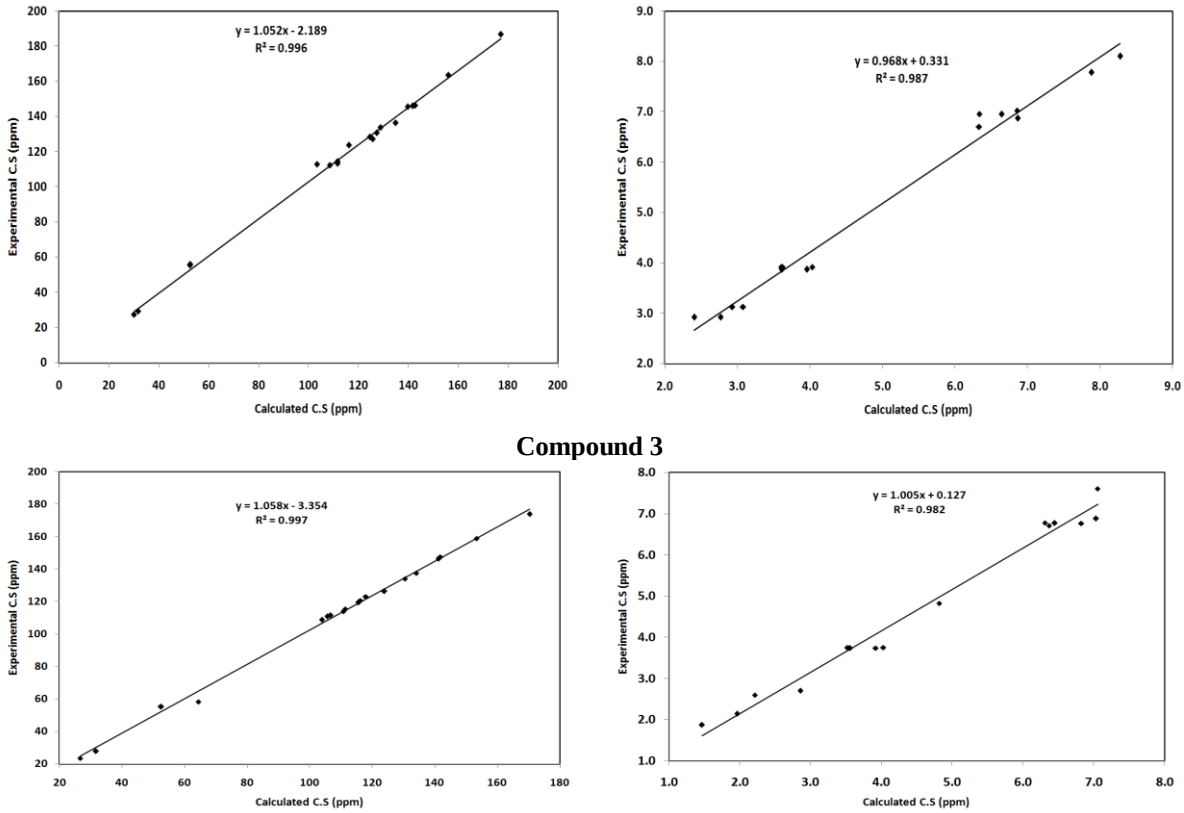

Fig. 5: Correlation between the calculated and experimental ^{13}C-(left) and ^{1}H-(right) NMR chemical shifts of the most stable isomers of 3 and 5. Note that H39, H41 and H43 chemical shifts of 5 were omitted from the correlation because these labile protons won't be computed satisfactorily because of the possibility of the strong interactions with solvent molecules.

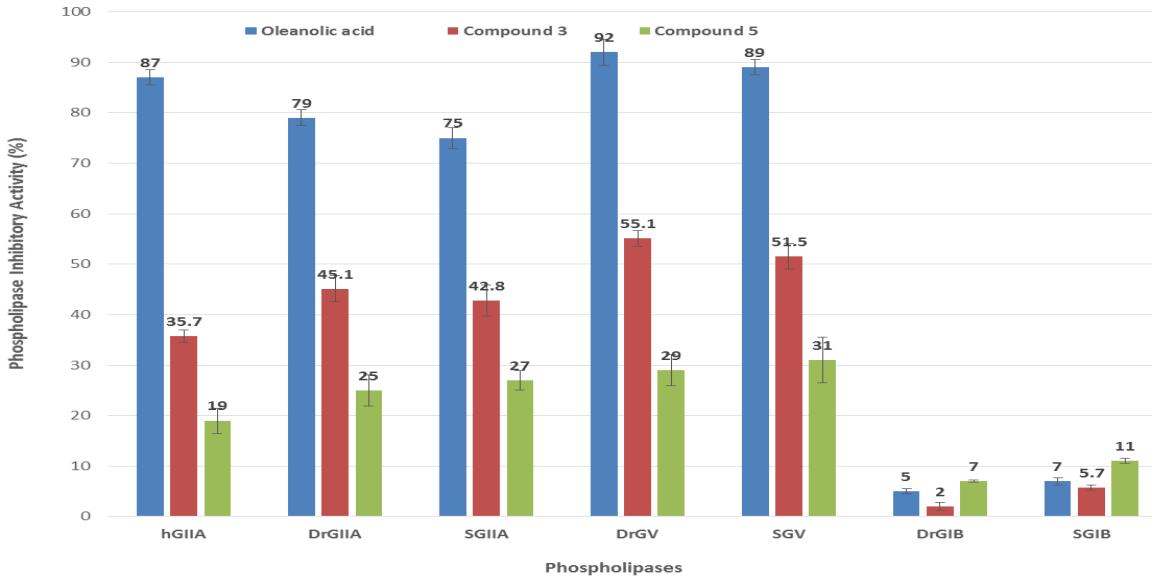

Fig. 6: Inhibitory effects of compounds 3 and 5 on 7 different sPLA$_2$s (hGIIA, DrGIIA, SGIIA, SGV, DrGIB and SG-IB) enzyme activities. Oleanolic acid was used as positive control. Experiments were performed in triplicate and are reported as the mean ± standard deviation.

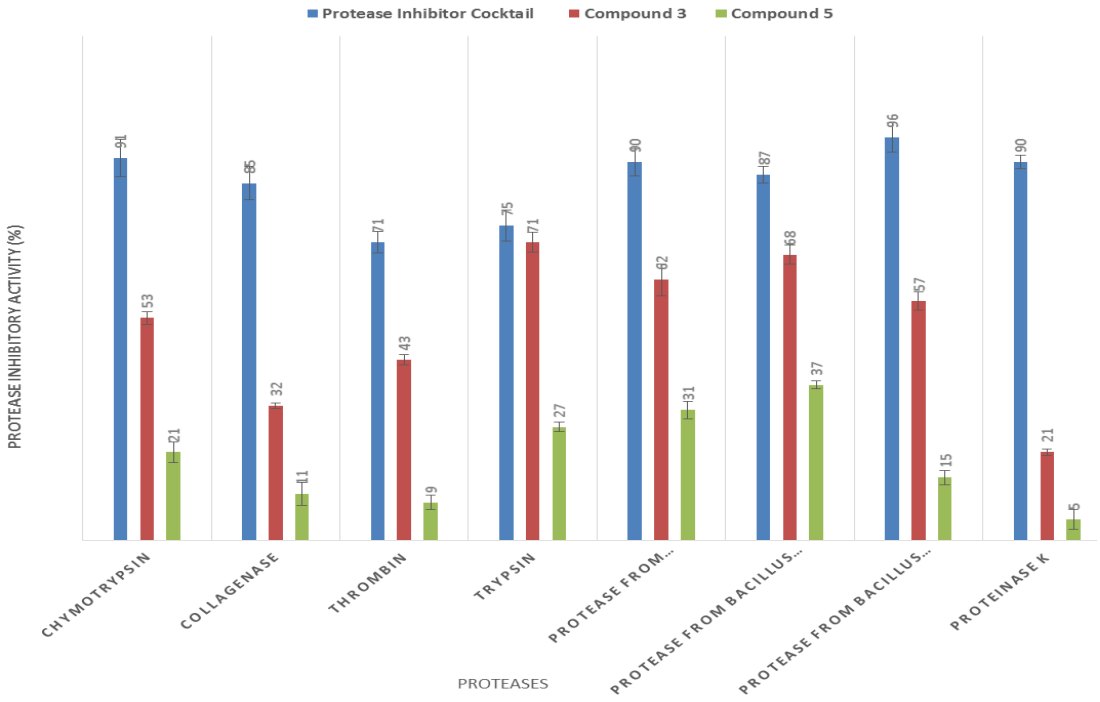

Fig. 7: Inhibitory activities of compounds 3 and 5 toward different pharmaceutically and commercially important proteases. Protease Inhibitor Cocktail (I3911 SIGMA) was used as positive control. Data are means of triplicate determinations ± SD.

Proteases inhibitory screening

Analogously, compounds **3** and **5** were examined for their anti-proteases activity against four of the commercially available proteases, namely, proteinase K and those obtained from *Aspergillus oryzae*, *Bacillus licheniformis* and *Bacillus sp.*, and four other therapeutically important proteases including chymotrypsin, collagenase, thrombin and trypsin. The screening results are shown in Fig 7 reveal that 2-arylidenetetralin-1-one **3** was more effective than compound **5** towards all of the tested proteases with its maximum inhibitory activity against trypsin (71 %), as compared to that of the reference protease inhibitor; cocktail (75 %). The weakest inhibition was recorded against proteinase K (21 %) as compared to cocktail (90 %).

Considering the large number of *in vitro* and *in vivo* reports indicated that active trypsin is one component of the multifaceted response of the acute inflammatory diseases of the pancreas [63], and its activity was also increased in tissues from patients with Crohn's disease and ulcerative colitis [64], compound **3** may be considered as a potential candidate that can be chemically modified to enhance its inhibitory potency for the treatment of such acute inflammatory disorders.

Antimicrobial screening

Moreover, compounds **3** and **5** were further screened for *in vitro* antimicrobial activities against two pathogenic plant fungi, namely, *Fusarium sp.* and *Alternaria alternate* as well as against fourteen strains of gram positive and gram negative bacteria. Screening results are presented in Table-7 and 8. As shown in Table-7, both compounds are capable of inhibiting the growth of the tested fungi and are found to be more effective against the fungus *Fusarium sp.* than *Alternaria alternate*. Moreover, compound **3** has a higher inhibitory effect by displaying the smallest diameter for fungal growth (29 mm) in comparison to both of compound **5** (33 mm), and the control Petri dish of the tested fungi with full fungal growth.

Table-7: Antifungal properties of compounds 3 and 5 against two pathogenic plant fungi.

	Alternaria alternata	***Fusarium sp.***

Control	Comp 3	Comp 5	Control	Comp 3	Comp 5
Full growth	29 mm	33 mm	Full growth	39 mm	38 mm

The antifungal effect of studied compounds (100 µg) was assessed by measuring the growth of each fungal strain and expressed as the mean diameter growth in mm. DMSO was used as the negative control.

Table-8: Antibacterial properties of compounds 3 and 5 expressed in inhibition zones (mm) against several Gram-positive and Gram-negative bacteria.

Organisms	Comp. 3 Average inhibition zone in (mm)	Comp. 5 Average inhibition zone in (mm)	Positive control Standard discs inhibition zone in (mm)		
			TE (30µg)	V (30µg)	CE (120µg)
***Stapylococcus aureus* ATCC 25923**	**10±0.2**	**-**	**32**	**-**	**-**
Ala1	**-**	**-**	**29**	**-**	**-**
MRSA ATCC 3345	**10±0.1**	**-**	**-**	**20**	**-**
MRSA	**-**	**-**	**-**	**19**	**-**
Streptococcus pyogenes ATCC 19615	**10±0.2**	**-**	**23**	**-**	**-**
Streptococcus mutans	**18.5±0.1**	**-**	**29**	**-**	**-**
Entrococcus feacalis ATCC 29212	**-**	**-**	**8**	**-**	**-**
Bacillus subtilis ATCC 6633	**10±0.1**	**-**	**12**	**-**	**-**
Escherichia coli ATCC25922	**-**	**-**	**19**	**-**	**-**
Escherichia coli ATCC	**-**	**-**	**20**	**-**	**-**
Pseudomonas aeruginosa ATCC 27853	**13±0.1**	**-**	**-**	**-**	**29**
Klebsiella pneumoniae ATCC 700603	**12±0.1**	**-**	**-**	**-**	**26**
Salmonella sp.	**8±0.1**	**-**	**23**	**-**	**-**
LT2	**-**	**-**	**20**	**-**	**-**
Serratia marscens	**13.5±0.3**	**-**	**13**	**-**	**-**

The bactericidal effect of studied compounds was assessed by measuring the diameter of inhibition zone (70 µg/well). Tetracycline (TE), Vancomycin (VA) and Gentamicin (CN) were used as the positive reference standards, and DMSO was used as the negative control.

The results of antibacterial screening shown in Table-8 reveal that while tetrahydrobenzo[*h*]quinazoline-2-thione derivative **5** is completely inactive, 2-arylidenetetralin-1-one **3** demonstrates moderate to good antibacterial activity against both gram positive and gram negative bacteria. The highest inhibitory effects of compound **3** are observed against gram positive *Streptococcus mutans* (18 mm) followed by gram negative bacterial strains namely; *Serratia marscenses* (13.5 mm), *Pseudomonas aeruginosa* (13 mm), *Klebsiella pneumoniae* (12 mm), *Staphylococcus aureus*, MRSA and *Bacillus subtilis*all by displaying an inhibition zone of 10 mm; however, lower effects are observed against *Salmonella sp*. (8 mm), in addition to bacterial strains; *Ala, Entrococcus feacalis ATCC 29212, E .coli* and LT2 (*Salmonella typhimurium*) are completely unaffected by the tested compounds.

Table-9: Antibacterial activities of compound 3 expressed in terms of IC_{50} and MIC.

Organisms	IC_{50} (µg/mL)	MIC (µg/mL)
***Stapylococcus aureus* ATCC 25923**	**2250±50**	**>970**
MRSA ATCC 3345	**1450±75**	**>620**
Streptococcus pyogenes ATCC 19615	**1650±45**	**>850**
Streptococcus mutans	**2500±100**	**>1050**
Bacillus subtilis ATCC 6633	**1500±70**	**>620**
Pseudomonas aeruginosa ATCC 27853	**2180±80**	**>560**
Klebsiella pneumoniae ATCC 700603	**1200±80**	**>780**
Salmonella sp.	**1450±40**	**>890**
Serratia marscens	**2070±30**	**>1100**

IC_{50}, the compound concentration necessary to kill 50% of the initial inoculum, was deduced from curves obtained from three independent experiments. MIC values represent the lowest concentrations of the studied chemical compounds which are capable of completely inhibiting the visible growth of bacteria. DMSO was used as the negative control

In the view of the obtained results of the antibacterial activities, the IC_{50} value, i.e. the compound concentration necessary to kill 50% of the initial inoculum, which was deduced from curves obtained from three independent experiments and MIC (the minimal inhibitory concentration) value i.e. the lowest compound concentrations that completely inhibited the growth of microorganisms were determined for compound **3** (Table-9) towards the more sensitive microbes. These experiments indicate that compound **3** displayed the lowest IC_{50} against gram negative *Klebsiella pneumoniae ATCC 700603.*

Conclusions

In this study, 2-(4-hydroxy-3-methoxy-benzylidene)-6-methoxy-3,4-dihydro-2*H*-naphthalen-1-one **3** and 4-(4-hydroxy-3-methoxy-phenyl)-8-methoxy-3,4,5,6-tetrahydro-1*H*-benzo[*h*]quinazoline-2-thione **5** were synthesized and their molecular structures were confirmed using different spectroscopic analyses and DFT computations. The relative stabilities of their suggested isomers were discussed in the framework of the DFT/B3LYP method. The most stable isomer for compound **3** was found to be the one that was observed experimentally using X-ray diffraction. The frontier molecular orbitals of the most stable isomers were also calculated and discussed. The energies of the HOMO and LUMO orbitals were taken as indicators of the ability of the molecules to donate and accept electrons respectively. The NMR spectral data of the stable isomers was well correlated with the experimental NMR chemical shifts. Antiphospholipases and antiproteases testing revealed that compound **3** was more active than **5** against all the tested enzymes except for the two isoforms of GIB $sPLA_2$s, as compound **5** showed

higher inhibition even than the that of oleanolic acid which is used as the reference phospholipases inhibitor. Thereby, compound **5** might serve as a potential candidate for treatment of diet induced obesity and diabetes. Furthermore, antibacterial screening showed that enone **3** was more potent and displayed the lowest IC_{50} against gram negative *Klebsiella pneumoniae ATCC 700603*.

Acknowledgments

The authors extend their appreciation to the Deanship of Scientific Research at King Saud University for funding this work through research group No **(**RG-1435-083**)**

Conflicts of Interest

The authors declare no conflict of interest regarding the publication of this paper.

References

1. M. Murakami, Y. Taketomi, H. Sato, K. Yamamoto, Secreted phospholipase A_2 revisited, *J. Biochem.*, **150**, 233 (2011).
2. H. Sato, Y. Taketomi and M. Murakami, Metabolic regulation by secreted phospholipase A_2, *Inflamm Regen.*, **36**, 7 (2016).
3. T. L. Tan, Y. Y. Goh, The role of group IIA secretory phospholipase A2 (sPLA2-IIA) as a biomarker for the diagnosis of sepsis and bacterial infection in adults—A systematic review, *PLoS ONE.*, **12**, e0180554 (2017).
4. C. Zhang, H. Yu, H. Xu, L. Yang, Expression of secreted phospholipase A2-Group IIA correlates with prognosis of gastric adenocarcinoma, *Oncol Lett.*, **10**, 3050 (2015**)**.
5. M. Menschikowski, A. Hagelgans, E. Gussakovsky, H. Kostka, E. L. Paley, G. Siegert, Differential expression of secretory phospholipases A_2 in normal and malignant prostate cell lines: Regulation by cytokines, cell signaling pathways, and epigenetic mechanisms, *Neoplasia*, **10**, 279 (2008).
6. G. S. D. Moses, M. D. Jensen, L. F. Lue, D. G. Walker, A. Y. Sun, A. Simonyi, G. Y. Sun, Secretory PLA_2-IIA: a new inflammatory factor for Alzheimer's disease, *J. Neuroinflammation*, **3**, 28 (2006).
7. D. Divchev, B. Schieffer, The secretory phospholipase A_2 group IIA: a missing link between inflammation, activated renin-angiotensin system, and atherogenesis?, *Vasc. Health Risk Manag.*, **4**, 597 (2008).
8. K. W. Huggins, A. C. Boileau, D. Y. Hui, Protection against diet-induced obesity and obesity- related insulin resistance in Group 1B PLA_2-deficient mice, *Am J Physiol Endocrinol Metab.*, **283**, E994 (2002).
9. C. López-Otín, J. S. Bond, Proteases: Multifunctional Enzymes in Life and Disease, *J. Biol. Chem.*, **283**, 30433 (2008).
10. J. Kryczka, J. Boncela, Proteases Revisited: Roles and Therapeutic Implications in Fibrosis, *Mediators Inflamm.*, **2017**, 1 (2017).
11. A. Falanga, L. Russo, V. Milesi, A. Vignoli, Mechanisms and risk factors of thrombosis in cancer, *Crit Rev Oncol Hematol.*, **118**, 79 (2017).
12. L. E. Hillebrand, F. Bengsch, J. Hochrein, J. Hülsdünker, J. Bender, M. Follo, H. Busch, M. Boerries, T. Reinheckel, Proteolysis–a characteristic of tumor-initiating cells in murine metastatic breast cancer, *Oncotarget.*, 58244 (2016).
13. S. T. Philominathan, O. Matsushita, R. Gensure, J. Sakon, Ca2+-induced linker transformation leads to a compact and rigid collagen-binding domain of Clostridium histolyticum collagenase. *FEBS J.*, **276**, 3589 (2009).
14. J. Peregrina-Sandoval, S. D. Toro-Arreola, A. Oceguera-Villanueva, F. Cerda-Camacho, A. D. Toro-Arreola, O. R. Gonzalez-Ramella, J. Jesse-Haramati, A. Daneri-Navarro, Trypsin proteolytic activity in cervical cancer and precursor lesions. *Int J Clin Exp Pathol*., **10**, 5587 (2017).
15. L. de S. Ramos, L. S. Barbedo, L. A. Braga-Silva, A. L. dos Santos, M. R. Pinto, D. B. Sgarbi, Protease and phospholipase activities of Candida spp. isolated from cutaneous candidiasis, *Rev Iberoam Micol.*, **32**, 22 (2015).
16. J. A. Yu, S. Kalatardi, J. Dohse, M. R. Sadaria, X. Meng, D. A Fullerton, M. J. Weyant, Group IIa sPLA2 inhibition attenuates NF-kB activity and promotes apoptosis in lung cancer cells, *Anticancer Res.*, **32**, 3601 (2012).
17. J. D. Bradley, A. A. A. J. Dmitrienko, Kivitz, O. S. Gluck, A. L. Weaver, C. Wiesenhutter, S. L. Myers, G. D. Sides, A randomized, double-blinded, placebo-controlled clinical trial of LY333013, a selective inhibitor of group II secretory phospholipase A2, in the treatment of rheumatoid arthritis, *J. Rheumatol.*, **32**, 417 (2005).
18. S. R. A. Leite, Inhibitors of Clostridium histolyticum collagenase, *Ecl. Quím., São Paulo*., **33**, 47 (2008).
19. E. T. Alexander, A. R. Minton, M. C. Peters, J. van Ryn, S. K. Gilmour, Thrombin inhibition

and cisplatin block tumor progression in ovarian cancer by alleviating the immunosuppressive microenvironment, *Oncotarget.*, **20**, 85291 (2016).

20. L. Schoofs, E. Clynen, M. Salzet, Trypsin and Chymotrypsin Inhibitors in Insects and Gut Leeches, *Curr Pharm Des.*, **8**, 483 (2002).
21. A. Juhem, A. Boumendjel, B. Touquet, A. Guillot, A. Popov, X. Ronot, V. Martel-Frachet, AG11, A Novel Dichloroflavanone Derivative with Anti-mitotic Activity Towards Human Bladder Cancer Cells, *Anticancer Res.*, **33**, 4445 (2013).
22. A. Gómez-Rivera, H. Aguilar-Mariscal, N. Romero-Ceronio, L. F. Roa-de la Fuente, C. E. Lobato-García, Synthesis and anti-inflammatory activity of three nitro chalcones, *Bioorg. Med. Chem. Lett.*, **23**, 5519 (2013).
23. T. Doan, D. T. Tran, Synthesis, Antioxidant and Antimicrobial Activities of a Novel Series of Chalcones, Pyrazolic Chalcones, and Allylic Chalcones, *Pharmacol. Pharm.* **2**, 282 (2011).
24. K. R. A. Abdellatif, H. A. H. Elshemy, S. A. Salama, H. A. Omar, Synthesis, characterization and biological evaluation of novel 4'-fluoro-2'-hydroxy-chalcone derivatives as antioxidant, anti-inflammatory and analgesic agents, *J. Enzyme Inhib. Med. Chem.*, **30**, 484 (2015).
25. M. Bonesi, M. R. Loizzo, G. A. Statti, S. Michel, F. Tillequin, F. Menichini, The synthesis and Angiotensin Converting Enzyme (ACE) inhibitory activity of chalcones and their pyrazole derivatives, *Bioorg. Med. Chem. Lett.*, **20**, 1990 (2010).
26. D. Desta, R. Sjoholm , L. Lee, M. Lee, K. Dittenhafer, S. Canche, B. Babu, S. Chavda, C. Dewar, S. Yanow, A. A. Best, M. Lee, Synthesis and antiprotozoal activity of 1,2,3,4-tetrahydro-2-thioxopyrimidine analogs of combretastatin A-4, *Med. Chem. Res.*, **20**, 364 (2010).
27. Y. R. Prasad, S. A. Rahaman, Anti-histamine activity of newly synthesized pyrimidines, *Int. J. Chem. Sci.*, **6**, 2038 (2008).
28. X. Fang, B. Yang, Z. Cheng, P. Zhang, M. Yang, Synthesis and antimicrobial activity of novel chalcone derivatives, *Res. Chem. Intermed.*, **40**, 1715 (2014).
29. L. S. Ming, J. Jamalis, H. M. Al-Maqtari, M. M. Rosli, M. Sankaranarayanan, S. Chander, H. Fun, Synthesis Characterization, Antifungal Activities and Crystal Structure of Thiophene-based Heterocyclic Chalcones, *Chemical Data Collections*, **9**, 104 (2017).
30. Z. Qi, M. Liu, Y. Liu, M. Zhang, G. Yang, Tetramethoxychalcone, a chalcone derivative, suppresses proliferation, blocks cell cycle progression, and induces apoptosis of human ovarian cancer cells, *PLoS ONE.*, **9**, e106206 (2014).
31. Y. Feng, X. Ding, T. Chen, L. Chen, F. Liu, X. Jia, X. Luo, X. Shen, K. Chen, H. Jiang, H. Wang, H. Liu, D. Liu, Design, synthesis, and interaction study of quinazoline-2(1*H*)-thione derivatives as novel potential Bcl-x_L inhibitors, *J. Med. Chem.*, **53**, 3465 (2010).
32. N. Raghav, M. Singh, Design, synthesis and docking studies of bischalcones based quinazoline-2(1H)-ones and quinazoline-2(1H)-thiones derivatives as novel inhibitors of cathepsin B and cathepsin H, *Eur. J. Pharm. Sci.*, **54**, 28 (2014).
33. R. Gali, J. Banothu, M. Porika, R. Velpula, S. Hnamte, R. Bavantula, S. Abbagani, S. Busi, Indolylmethylene benzo[h]thiazolo[2,3-b]quinazolinones: Synthesis, characterization and evaluation of anticancer and antimicrobial activities, *Bioorg. Med. Chem. Lett.*, **24**, 4239 (2014).
34. L. M. Antypenko, S. I. Kovalenko, O. M. Antypenko, A. M. Katsev, O. M. Achkasova, Design and evaluation of novel antimicrobial and anticancer agents among tetrazolo [1,5-*c*]quinazoline-5-thione S-derivatives, *Sci. Pharm.*, **81**, 15 (2013).
35. Y. A. Mohamed, A. EG. E. Amr, S. F. Mohamed, M. M. Abdalla, M. A. Al-Omar, S. H. Shfik, Cytotoxicity and anti-HIV evaluations of some new synthesized quinazoline and thioxopyrimidine derivatives using 4-(thiophen-2-yl)-3,4,5,6-tetrahydrobenzo[h]quinazoline-2(1H)-thione as synthons, *J. Chem. Sci.*, **124**, 693 (2012).
36. N. N. E. El-Sayed, A. M. Alafeefy, M. A. Bakhit, V. H. Masand, A. Aldalbahi, N. Chen, C. Fan, A. Ben Bacha, Synthesis, Antiphospholipase A_2, Antiprotease, Antibacterial Evaluation and Molecular Docking Analysis of Certain Novel Hydrazones, *Molecules*, **21**, 1664 (2016).
37. N. N. E. El-Sayed, N. A. AL-Balawi, A. M. Alafeefy, M. A. AL-ALShaikh**,** K. M. Khan, Synthesis, characterization and antimicrobial evaluation of some thiazole derived carbamates, semicarbazones, amides and carboxamide, *J. chem. Soc. Pak.*, **38**, 358 (2016).
38. Z. Y. Du, R. Liu, W. Shao, X. Mao, L. Ma, L. Gu, Z. Huang, A. S. Chan, C. α-Glucosidase Inhibition of Natural Curcuminoids and Curcumin Analogs, *Eur J Med Chem.*, **41**, 213 (2006).

39. A. D. Becke, Density-functional thermochemistry. III. The role of exact exchange, *J. Chem. Phys.*, **98**, 5648 (1993).
40. C. Lee, W. Yang, R. G. Parr, Development of the Colle-Salvetti correlation-energy formula into a functional of the electron density, *Phys. Rev. B*, **37**, 785 (1988).
41. M. J. Frisch, H. B. Trucks, G. E. Schlegel, M. A. Scuseria, Robb, et al, Gaussian-03, Revision C.01, Gaussian, Inc., Wallingford, CT, 2004.
42. R. Dennington II, T. Keith, J. Millam, Gauss View, Version 4.1, Semichem Inc., Shawnee Mission, KS, 2007.
43. T. L. Hill, In *Introduction to Statistic Thermodynamics*, Addison-Wesley Publishers, New York (1960). https://doi.org/10.1002/bbpc.19620660121.
44. R. Ditchfield, Molecular orbital theory of magnetic shielding and magnetic susceptibility. *J. Chem. Phys.*, **56**, 5688 (1972).
45. K. Wolinski, Hinton, J. F.; Pulay, P. Efficient implementation of the gauge-independent atomic orbital method for NMR chemical shift calculations. *J. Am. Chem. Soc.*, **112**, 8251 (1990).
46. J. Chocholoušová, V. Špirko, P. Hobza, First local minimum of the formic acid dimer exhibits simultaneously red-shifted O-H...O and improper blue-shifted C-H…O hydrogen bonds, *Phys. Chem. Chem. Phys.*, **6**, 37 (2004).
47. A. Lōbo de Araújo, F. Radvanyi, Determination of phospholipase A_2 activity by a colorimetric assay using a pH indicator, *Toxicon.*, **25**, 1181 (1987).
48. M. Kunitz, Crystalline soyabean trypsin inhibitor: II. General properties, *J. Gen. Physiol.*, **30**, 291 (1947).
49. D. A. vanden Berghe, A. J. Vlietinck, In *Methods in Plant Biochemistry (Assays for bioactivity)* Screening methods for antibacterial and antiviral agents from higher plants, Hostettmann K., (Eds), volume 6, Academic Press, London, p. 47 (1991).
50. D. Wade, A. Silveira, L. Rollins-Smith, T. Bergman, J. Silberring, H. Lankinen, Hematological and antifungal properties of temporin A and a cecropin A-temporin A hybrid, *Acta Biochim. Pol.*, **48**, 1185 (2001). PMID: 11995990.
51. Ö. Ertürk, Antimicrobial Activity of Viscum album L. subsp. abietis (Wiesb), *Turk. J. Biol.*, **27**, 255 (2003).
52. U. W. Hawas, M. A. Al-Omar, A. G. E. Amr, A. E-F. G. Hammam, Synthesis of some thiopyrimidine and thiazolopyrimidines starting from 2,6-dibenzylidene-3-methylcyclohexanone and its antimicrobial activities, *Arab. J. Chem.*, ***5***, 509 (2012).
53. B. Kaur, R. Kaur, Synthesis of fused quinazolinethiones and their S-alkyl/aryl derivatives, *Arkivoc*, **xv**, 315 (2007).
54. C. O. Kappe, A Reexamination of the Mechanism of the Biginelli Dihydropyrimidine Synthesis. Support for an N-Acyliminium Ion Intermediate, *J. Org. Chem.*, **62**, 7201 (1997).
55. N. N. E. El-Sayed, N. M. Almaneai, H. A. Ghabbour, A. M. Alafeefy, Crystal structure of (E)-2-(4-hydroxy-3-methoxybenzylidene)-6-methoxy-3,4-dihyronaphthalene-1(2H)- one, C19H18O4, *Z. Kristallogr. NCS.*, **232**, 203 (2017).
56. R. G. Parr, L. Szentpaly, S. Liu, Electrophilicity Index, *J. Am. Chem. Soc.*, **121** 1922 (1999).
57. P. K. Chattaraj, B. Maiti, U. Sarkar, Philicity: A Unified Treatment of Chemical Reactivity and Selectivity, *J. Phys. Chem. A*, **107**, 4973 (2003).
58. R. G. Parr, R. A. Donnelly, M. Levy, W. E. Palke, Electronegativity: The density functional viewpoint, *J. Chem. Phys.*, **68**, 3801 (1978).
59. R.G. Parr, R.G. Pearson, Absolute hardness: companion parameter to absolute electronegativity, *J. Am. Chem. Soc.*, **105**, 7512 (1983).
60. R. G. Parr, P. K. Chattraj, Principle of maximum hardness, *J. Am. Chem. Soc.*, **113**, 1854 (1991) DOI: 10.1021/ja00005a072.
61. R. G. Parr and R. G. Pearson, Absolute hardness: companion parameter to absolute electronegativity, *J. Am. Chem. Soc.* **105**, 7512 (1983).
62. A. Barakat, M. Ali, S. M. Soliman, A. M. Abu-Elfotoh, A. M. Al-Majid, H. A. Ghabbour, New hybrid of the barbituric acid motif: synthesis, X-ray single crystal, DFT, and Hirshfeld surface analyses, *Research on Chemical Intermediates*, 1 (2018).
63. J. I. Baoan, C. D. Logsdon, Digesting new information about the role of trypsin in pancreatitis, *Gastroenterology*, **141**, 1972 (2011).
64. N. Cenac, C. N. Andrews, M. Holzhausen, K. Chapman, G. Cottrell, P. Andrade-Gordon, M. Steinhoff, G. Barbara, P. Beck, N. W. Bunnett, K. A. Sharkey, J. G. P. Ferraz, E. Shaffer, N. Vergnolle, Role for protease activity in visceral pain in irritable bowel syndrome, *J. Clin. Invest.*, **117**, 636 (2007).